Article

A Supramolecular Receptor of Diatomic Molecules (O, CO, NO) in Aqueous Solution

Koji Kano, Yoshiki Itoh, Hiroaki Kitagishi, Takashi Hayashi, and Shun Hirota

More About This Article

Additional resources and features associated with this article are available within the HTML version:

- Supporting Information
- Access to high resolution figures
- Links to articles and content related to this article
- Copyright permission to reproduce figures and/or text from this article

View the Full Text HTML

A Supramolecular Receptor of Diatomic Molecules (O₂, CO, NO) in Aqueous Solution

Koji Kano,*,† Yoshiki Itoh,† Hiroaki Kitagishi,§ Takashi Hayashi,§ and Shun Hirota‡

Department of Molecular Science and Technology, Faculty of Engineering, Doshisha University, Kyotanabe, Kyoto 610-0321, Japan, Department of Applied Chemistry, Graduate School of Engineering, Osaka University, Suita, Osaka 562-0014, and Graduate School of Material Sciences, Nara Institute of Science and Technology, Ikoma, Nara 630-0192, Japan

Received February 7, 2008; E-mail: kkano@mail.doshisha.ac.jp

Abstract: A per-*O*-methylated β-cyclodextrin dimer, Py2CD, was conveniently prepared via two steps: the Williamson reaction of 3,5-bis(bromomethyl)pyridine and β-cyclodextrin (β-CD) yielding 2*A*,2′*A*-*O*-[3,5-pyridinediylbis(methylene)bis-β-cyclodextrin (bisCD) followed by the *O*-methylation of all the hydroxy groups of the bisCD. Py2CD formed a very stable 1:1 complex (Fe(III)PCD) with [5,10,15,20-tetrakis(*p*-sulfonatophenyl)porphinato]iron(III) (Fe^{III}TPPS) in aqueous solution. Fe(III)PCD was reduced with Na₂S₂O₄ to afford the Fe^{II}TPPS/Py2CD complex (Fe(II)PCD). Dioxygen was bound to Fe(II)PCD, the $P_{1/2}^{O2}$ values being 42.4 ± 1.6 and 176 ± 3 Torr at 3 and 25 °C, respectively. The k_{on}^{O2} and k_{off}^{O2} values for the dioxygen binding were determined to be 1.3×10^7 M^{-1}s^{-1} and 3.8×10^3 s^{-1}, respectively, at 25 °C. Although the dioxygen adduct was not very stable ($K_{O2} = k_{on}^{O2}/k_{off}^{O2} = 3.4 \times 10^3$ M^{-1}), no autoxidation of the dioxygen adduct of Fe(II)PCD to Fe(III)PCD was observed. These results suggest that the encapsulation of Fe^{II}TPPS by Py2CD strictly inhibits not only the extrusion of dioxygen from the cyclodextrin cage but also the penetration of a water molecule into the cage. The carbon monoxide affinity of Fe(II)PCD was much higher than the dioxygen affinity; the $P_{1/2}^{CO}$, k_{on}^{CO}, k_{off}^{CO}, and K_{CO} values being $(1.6 \pm 0.2) \times 10^{-2}$ Torr, 2.4×10^6 M^{-1}s^{-1}, 4.8×10^{-2} s^{-1}, and 5.0×10^7 M^{-1}, respectively, at 25 °C. Fe(II)PCD also bound nitric oxide. The rate of the dissociation of NO from (NO)Fe(II)PCD ($(5.58 \pm 0.42) \times 10^{-5}$ s^{-1}) was in good agreement with the maximum rate ($(5.12 \pm 0.18) \times 10^{-5}$ s^{-1}) of the oxidation of (NO)Fe(II)PCD to Fe(III)PCD and NO₃⁻, suggesting that the autoxidation of (NO)Fe(II)PCD proceeds through the ligand exchange between NO and O₂ followed by the rapid reaction of (O₂)Fe(II)PCD with released NO, affording Fe(II)PCD and the NO₃⁻ anion inside the cyclodextrin cage.

Introduction

The capture of diatomic molecules is an attractive research subject because some of these simple molecules play important roles in life processes as well as in industrial reactions. The capture of dioxygen by metal complexes has been widely investigated in relation to biological dioxygen transport and storage[1] as well as to dioxygen activation.[2] A picket-fence porphyrin is the typical ferrous complex as a myoglobin (Mb) model that reversibly binds dioxygen in toluene.[3] Nonheme dinuclear copper complexes have also been prepared as the models of the dioxygen transport protein, hemocyanin.[4] These metal complexes with dioxygen affinities usually bind carbon monoxide and nitric oxide which are biologically important diatomic molecules. However, the focus of the traditional functional models has mainly been directed to the prosthetic groups of the proteins, and little attention has been paid to the apoproteins. The supramolecular characteristics of the native dioxygen-receiving proteins, such as Mb, Hb, and hemocyanin, are achieved only by the cooperative action between the prosthetic groups and the apoproteins. A model system without the apoprotein-mimetic functionality generally shows a very limited function of the intended holoprotein. For example, the picket-fence porphyrins as well as the metalloporphyrins prepared on the basis of the same concept as the picket-fence porphyrins[5] bind dioxygen only in organic solvents, and the dioxygen adducts of these models immediately decompose in the presence of a small amount of water. Although a few

† Doshisha University.
§ Osaka University.
‡ Nara Institute of Science and Technology.

(1) (a) Collman, J. P.; Boulatov, R.; Sunderland, C. J.; Fu, L. *Chem. Rev.* **2004**, *104*, 561–588. (b) Trayler, T. G. *Acc. Chem. Res.* **1981**, *14*, 102–109.

(2) For examples: Nam, W. *Acc. Chem. Res.* **2007**, *40*, 522–531. (b) Groves, J. T. *J. Inorg. Biochem.* **2006**, *100*, 434–447. (c) Decker, A.; Solomon, E. I. *Curr. Opinion Chem. Biol.* **2005**, *9*, 152–163. (d) Karlin, K. D.; Lee, D.-H.; Obias, H. V.; Humphreys, K. J. *Pure Appl. Chem.* **1998**, *70*, 855–862.

(3) (a) Collman, J. P.; Gagne, R. R.; Halbert, T. R.; Marchon, J.-C.; Reed, C. A. *J. Am. Chem. Soc.* **1973**, *95*, 7868–7870. (b) Collman, J. P. *Acc. Chem. Res.* **1977**, *10*, 265–272.

(4) (a) Karlin, K. D.; Cruse, R. W.; Gultheh, Y.; Farooq, A.; Hayes, J. C.; Zubieta, J. *J. Am. Chem. Soc.* **1987**, *109*, 2668–2679. (b) Kitajima, N.; Fujisawa, K.; Fujimoto, C.; Morooka, Y.; Hashimoto, S.; Kitagawa, T.; Toriumi, K.; Tatsumi, K.; Nakamura, A. *J. Am. Chem. Soc.* **1992**, *114*, 1277–1291. (c) Kodera, M.; Katayama, K.; Tachi, Y.; Kano, K.; Hirota, S.; Fujinami, S.; Suzuki, M. *J. Am. Chem. Soc.* **1999**, *121*, 11006–11007.

(5) Momenteau, M.; Reed, C. A. *Chem. Rev.* **1994**, *94*, 659–698.
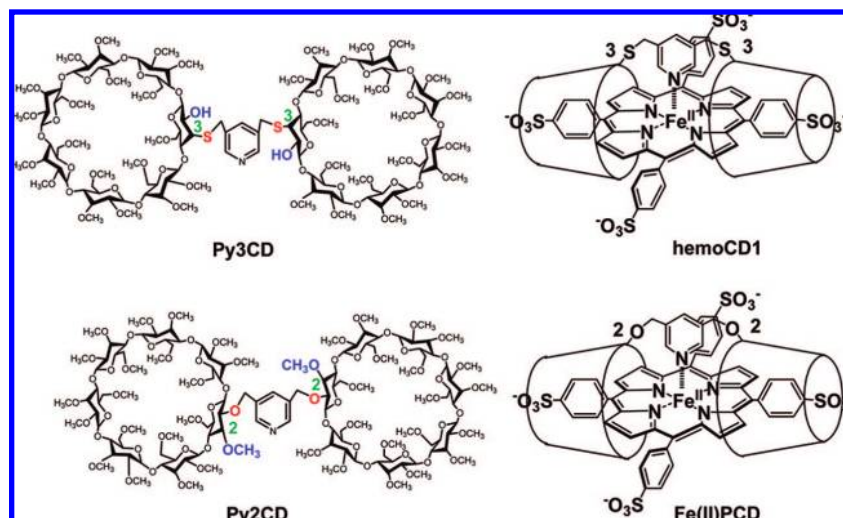
Figure 1. Structures of Py3CD, Py2CD, hemoCD1, and Fe(II)PCD.

attempts have been carried out to capture dioxygen by the artificial ferrous porphyrins in aqueous media, no stable dioxygen adducts have been obtained.[6] The instability of the dioxygen adducts in the model systems is mainly ascribed to the autoxidation of the oxygenated ferrous porphyrins promoted by a water molecule.[7,8] On the basis of the previous results, we can conclude that separation of the Fe(II) center of a model heme from the aqueous bulk phase is essential to achieve dioxygen binding in an aqueous solution. Until recently, no example has been reported with dioxygen binding to the model heme in an aqueous solution except for a picket-fence porphyrin in the liposomal membrane.[9] Quite recently, however, the dioxygen binding in an aqueous solution has been achieved by encapsulation of a water-soluble ferrous porphyrin, [5,10,15,20-tetrakis(*p*-sulfonatophenyl)porphinato]iron(II) (Fe^{II}TPPS), in a capsule formed by a cyclodextrin dimer (Py3CD, Figure 1).[8,10] The 1:1 complex of Fe^{II}TPPS and Py3CD is called hemoCD1 that reversibly binds dioxygen in an aqueous solution. Although hemoCD1 binds both dioxygen and carbon monoxide, it is decomposed by nitric oxide (Supporting Information). The sulfide bonds used for linking the two *O*-methylated β-cyclodextrin moieties probably participate in the decomposition of hemoCD1. We then tried to replace the sulfide bonds by the ether bonds. We simultaneously tried to shorten the synthetic steps for preparing the receptor of the diatomic molecules. The present paper deals with the convenient preparation of a new *O*-methylated β-cyclodextrin dimer (Py2CD, Figure 1) and the binding behavior of the 1:1 complex of Fe^{II}TPPS and Py2CD (Fe(II)PCD) for the diatomic molecules, such as dioxygen,

carbon monoxide, and nitric oxide. In the present study, we found the pronounced "cage effect" due to encapsulation of Fe^{II}TPPS in a capsule formed by the two cyclodextrin cavities of Py2CD upon binding of the diatomic molecules. We utilized such a phenomenon to define the mechanism for the oxidation of the nitric oxide adduct of Fe(II)PCD to Fe(III)PCD and NO$_3^-$. In this paper, we also report that the orientation of the proximal base (pyridine) is a very important factor for the affinities of the ferrous porphyrin to bind the diatomic molecules.

Experimental Section

Materials. Fe^{III}TPPS was the same as that used in a previous study.[11] Heptakis(2,3,6-tri-*O*-methyl)-β-cyclodextrin (TMe-β-CD, Nacalai) and other chemicals were purchased and used as received. Water was purified using a Millipore Simpak 1. Pure O$_2$ (99.999%), pure N$_2$ (99.999%), NO (99%), and diluted CO (0.0909% CO in N$_2$) gases were purchased from Sumitomo Seika Chemicals. The NO gas was used after passing it through a trap of KOH. ^{13}CO (ICON, ^{13}C 99 atom %) was used for the resonance Raman spectroscopic measurements.

2A,2′A-*O*-[3,5-Pyridinediyl-bis(methylene)bis-β-cyclodextrin (bisCD). A mixture of dried β-CD (7.1 g, 6.3 mmol) and NaOH (2.5 g, 63 mmol) in dry DMSO (40 mL) was stirred for 2 h at 55 °C under an Ar atmosphere. To this solution was added 3,5-bis(bromomethyl)pyridine hydrobromide (1.0 g, 2.9 mmol) in dry DMSO (15 mL), and the resulting mixture was stirred overnight. The reaction mixture was neutralized by dilute aqueous HCl, and the precipitates were collected by filtration. The filtrate was poured into a large amount of acetone (2 L), and the crude bisCD was filtered. The product was passed through a Diaion column with aqueous methanol (gradient) to purify bisCD. Yield 1.1 g (16%). ^{1}H NMR (400 MHz, D$_2$O): δ = 8.58 (s, 2 H), 8.10 (s, 1 H), 5.18 (s, 2 H), 5.09 (s, 12 H), 3.54−4.14 (m, 84 H). MS (MALDI-TOF, α-CHCA) *m/z*: calcd for [M + Na]$^+$ 2396.08; found 2396.

Py2CD. A mixture of bisCD (0.4 g, 0.17 mmol) and NaH (1.4 g, 58 mmol) in dry DMF (50 mL) was stirred for 1 h by cooling with ice, and then methyl iodide (1 mL, 7 mmol) was added to the solution. After stirring the mixture at room temperature overnight, the remaining NaH was decomposed with methanol, and the organic solvents were removed under reduced pressure. The residual solid was dissolved in a saturated aqueous NaCl solution and extracted with chloroform (100 mL × 5). Chloroform was evaporated until its volume was 100 mL, and the residual chloroform solution was

(6) (a) Jiang, D.-L.; Aida, T. *Chem. Commun.* **1996**, 1523–1524. (b) Zingg, A.; Felber, B.; Gramlich, V.; Fu, L.; Collman, J. P.; Diederich, F. *Helv. Chim. Acta* **2002**, *85*, 333–351.

(7) (a) Shikama, K. *Chem. Rev.* **1998**, *98*, 1357–1373. (b) Shikama, K. *Coord. Chem. Rev.* **1988**, *83*, 73–91. (c) Sugawara, Y.; Shikama, K. *Eur. J. Biochem.* **1978**, *91*, 407–413. (d) Sugawara, Y.; Shikama, K. *Eur. J. Biochem.* **1980**, *110*, 241–246. (e) Shikama, K.; Matsuoka, A. *Biochemistry* **1986**, *25*, 3898–3903.

(8) Kano, K.; Kitagishi, H.; Dagallier, C.; Kodera, M.; Matsuo, T.; Hayashi, T.; Hisaeda, Y.; Hirota, S. *Inorg. Chem.* **2006**, *45*, 4448–4460.

(9) (a) Tsuchida, E.; Nishide, H.; Yuasa, M.; Hasegawa, E.; Matsushita, Y. *J. Chem. Soc., Dalton Trans.* **1984**, 1147–1151. (b) Komatsu, T.; Moritake, M.; Nakagawa, A.; Tsuchida, E. *Chem. Eur. J.* **2002**, *8*, 5469–5480.

(10) Kano, K.; Kitagishi, H.; Kodera, M.; Hirota, S. *Angew. Chem., Int. Ed.* **2005**, *44*, 435–438.

(11) Kano, K.; Kitagishi, H.; Tamura, S.; Yamada, A. *J. Am. Chem. Soc.* **2004**, *126*, 15202–15210.

washed with aqueous sodium thiosulfate (100 mL). The chloroform layer was dried over Na_2SO_4, and then chloroform was evaporated. The solid residue was purified by silica gel column chromatography with chloroform−methanol (10: 1). Yield 0.1 g (25%). ^1H NMR (400 MHz, $CDCl_3$): δ = 8.65 (s, 2 H), 7.73 (s, 1 H), 4.85−5.16 (m, 12 H), 4.82−4.85 (d, 2 H), 4.63−4.66 (d, 2 H), 3.18−3.82 (m, 206 H). MS (FAB, m-NBA) m/z: calcd for $[M + H]^+$ 2935.16; found 2935. Elemental analysis (%) for $C_{131}H_{225}NO_{70} \cdot 2CHCl_3$: C, 50.35; H, 7.21; N, 0.44; O, 35.30; found: C, 50.43; H, 7.14; N, 0.49; O, 35.77.

Instruments. Most of the instruments used in this study were the same as previous ones. The EPR spectra (X-band) of the nitrosylated ferrous porphyrins were taken by a JEOL JES-TE200 ESR spectrometer at 77 K. The g-values were corrected using DPPH.

Preparation of O_2- and CO-Adducts of Fe(II)PCD. An excess amount of $Na_2S_2O_4$ (0.2 mg, 1.2×10^{-6} mol) was added to the 0.2 mL of Fe(III)PCD solution ($[Fe^{III}TPPS] = 3.0 \times 10^{-4}$ M, $[Py2CD] = 3.6 \times 10^{-4}$ M in 0.05 M phosphate buffer at pH 7.0). The resulting solution was charged to a Sephadex G-25 column (16×25 mm^2, superfine, HiTrap^{TM} desalting column, Amersham Biosciences) and eluted with the same buffer under aerobic conditions to remove the inorganic salts. During column chromatography, Fe(II)PCD partly changed to oxy-Fe(II)PCD. The obtained red-colored solution was diluted by the same buffer solution saturated with N_2 gas. Oxy-Fe(II)PCD was obtained by pouring the O_2 gas into the Fe(II)PCD solution at the appropriate temperature. The CO-adduct was easily obtained by introducing the CO gas into the oxy-Fe(II)PCD solution. The concentrations of Fe(II)PCD, oxy-Fe(II)PCD, and CO−Fe(II)PCD were determined by using the extinction coefficients of these compounds (vide infra).

Determination of O_2 and CO Affinities. The solution of Fe(II)PCD was prepared by the reduction of Fe(III)PCD with $Na_2S_2O_4$ in phosphate buffer at pH 7.0 and the subsequent removal of the inorganic salts by a Sephadex G-25 column. The O_2-N_2 mixed gas with a certain partial pressure was bubbled into the phosphate buffer solution (0.05 M, pH 7.0, 3 mL) in a quartz cell (10 mm optical length). After bubbling for at least 15 min, the stock solution of Fe(II)PCD was quickly added, and gentle bubbling was continued for an additional 3 min. The UV−vis spectra of Fe(II)PCD were measured as a function of the dioxygen partial pressure (P^{O2}). The change in absorbance (ΔA) of Fe(II)PCD upon binding with O_2 at P^{O2} is represented by eq 1:[12]

$$P^{O2} = \{\Delta\varepsilon[Fe(II)PCD]_t P^{O2}\}/\Delta A - P_{1/2}^{O2} \qquad (1)$$

where $\Delta\varepsilon$ is the difference in the extinction coefficients between Fe(II)PCD and oxy-Fe(II)PCD at a certain wavelength, $[Fe(II)PCD]_t$ is the initial concentration of Fe(II)PCD, and $P_{1/2}^{O2}$ is the partial O_2 pressure where half of the Fe(II)PCD molecules are oxygenated. The dioxygen affinity $P_{1/2}^{O2}$ was determined from the intercept of the linear plot of $P^{O2}/\Delta A$ vs P^{O2}.

The carbon monoxide affinity of Fe(II)PCD ($P_{1/2}^{CO}$) was also determined by the same procedure as that for dioxygen. The partial pressures of carbon monoxide were adjusted by the nitrogen gas.

Kinetic Measurements for O_2 and CO Binding. An excess amount of $Na_2S_2O_4$ was added to the 3×10^{-4} M Fe(III)PCD in 0.05 M phosphate buffer, and then the resulting solution was passed through a Sephadex G-25 column to remove the inorganic salts. The eluate involving only Fe(II)PCD was properly diluted by the same buffer solution. During the procedure, Fe(II)PCD bound dioxygen to some extent. After laser flash photolysis (λ_{ex} = 532 nm, 5 ns pulse) of (O_2)Fe(II)PCD at 25 °C, the rebinding of O_2 was monitored by following the change in the absorbance at 437 nm. The k_{obs}^{O2} values were measured at various partial dioxygen pressures, and the k_{on}^{O2} value was determined from the slope of a

linear relation between k_{obs}^{O2} and $[O_2]$ (Supporting Information). The k_{off}^{O2} value was calculated from eq 2:[13]

$$K^{O2} = (CP_{1/2}^{O2})^{-1} = k_{on}^{O2}/k_{off}^{O2} \qquad (2)$$

where C is the solubility of O_2 in water at 25 °C ($C = 1.67 \times 10^{-6}$ M Torr^{-1}).[14]

The mixture of Fe(II)PCD and (O_2)Fe(II)PCD in phosphate buffer (0.05 M, pH 7.0) was exposed to the carbon monoxide atmosphere, affording (CO)Fe(II)PCD. (CO)Fe(II)PCD was photolyzed by a laser flash, and the rebinding of carbon monoxide was monitored at 434 nm. The $P_{1/2}^{CO}$ value was so small that the k_{obs}^{CO} value was approximately equal to $k_{on}^{CO}[CO]$. The k_{off}^{CO} value was calculated from an equation corresponding to eq 2 ($C = 1.26 \times 10^{-6}$ M Torr^{-1}).[14]

Preparation of Nitric Oxide-Coordinate Fe(II)PCD and Kinetic Measurements for Oxidation. A 0.3 mL solution of a mixture of $Fe^{III}TPPS$ (3×10^{-4} M) and Py2CD (3.6×10^{-4} M) in 0.05 M phosphate buffer (pH 7.0) was bubbled using the nitric oxide gas for 10 s to afford (NO)Fe(II)PCD. The resulting (NO)Fe(II)PCD solution was passed through a Sephadex G-25 column. The eluate was appropriately diluted by the same buffer and the oxidation of (NO)Fe(III)PCD to Fe(III)PCD and NO_3^- was followed by measuring the change in the absorbance at 420 nm that is the λ_{max} of (NO)Fe(II)PCD.

Preparation of Nitric Oxide Adduct of $Mn^{II}TPPS$ Encapsulated by Py2CD and Kinetic Measurements for Oxidation. To a 0.2 mL solution of a mixture of $Mn^{III}TPPS$ (3×10^{-3} M) and Py2CD (3.6×10^{-3} M) in 0.05 M phosphate buffer (pH 7.0) was added $Na_2S_2O_4$ (5.7 μmol) to afford the $Mn(II)TPPS-Py2CD$ complex (Mn(II)PCD). The NO gas was gently blown over the surface of the Mn(II)PCD solution to produce (NO)Mn(II)PCD. The resulting solution was passed through a Sephadex G-25 column to remove any inorganic salts. The eluate was appropriately diluted by the same buffer, and the oxidation of (NO)Mn(II)PCD to Mn(III)PCD and NO_3^- was followed by the changes in the absorbances at 428 and 471 nm which were ascribed to (NO)Mn(II)PCD and Mn(III)PCD, respectively.

Results and Discussion

Preparation of Py2CD and Its Inclusion Complexes of FeTPPS. It has been reported that the Williamson reaction of 1,3-bis(bromomethyl)benzene with two equivalents of native β-CD affords 2A,2′A-O-1,3-phenylenebis(methylene)bis-β-CD in 10% yield.[15] We applied such a reaction to synthesize bisCD (16% yield) that was subsequently per-O-methylated by methyl iodide in DMF containing NaH to afford Py2CD (25% yield). No methylation occurred at the nitrogen of the pyridine moiety in the linker. Further study is needed with purification of bisCD. Impurities contained in bisCD made it difficult to purify the final product (Py2CD) by silica gel column chromatography.

The apparent pK_a value for the equilibrium between a diaqua complex of $Fe^{III}TPPS$ ($Fe^{III}TPPS(H_2O)_2$) and a μ-oxo-dimer of $Fe^{III}TPPS$ was reported to be 6.4.[16] Although most experiments in the present study were carried out at pH 7.0, the measurement of the binding constant (K) for complexation of $Fe^{III}TPPS$ with Py2CD was carried out in phosphate buffer at pH 8.0 in which the μ-oxo-dimer preferentially existed as the guest. Upon the addition of Py2CD, the absorption band at 408 nm due to the

(12) Collman, J. P.; Zhang, X.; Wong, K.; Brauman, J. I. *J. Am. Chem. Soc.* **1994**, *116*, 6245–6251.

(13) Collman, J. P.; Brauman, J. I.; Doxsee, K. M.; Sessler, J. L.; Morris, R. M.; Gibson, Q. H. *Inorg. Chem.* **1983**, *22*, 1427–1432.

(14) Wilhelm, E.; Battino, R.; Wilcock, R. J. *Chem. Rev.* **1977**, *77*, 219–262.

(15) Ishimaru, Y.; Iida, T. *Tetrahedron Lett.* **1997**, *38*, 3743–3744.

(16) Mosseri, S.; Mialocq, J. C.; Perly, B.; Hambright, P. *J. Phys. Chem.* **1991**, *95*, 4659–4663.

(17) Kitagishi, H. Ph.D. Dissertation, Doshisha University, Kyoto, Japan, 2006.
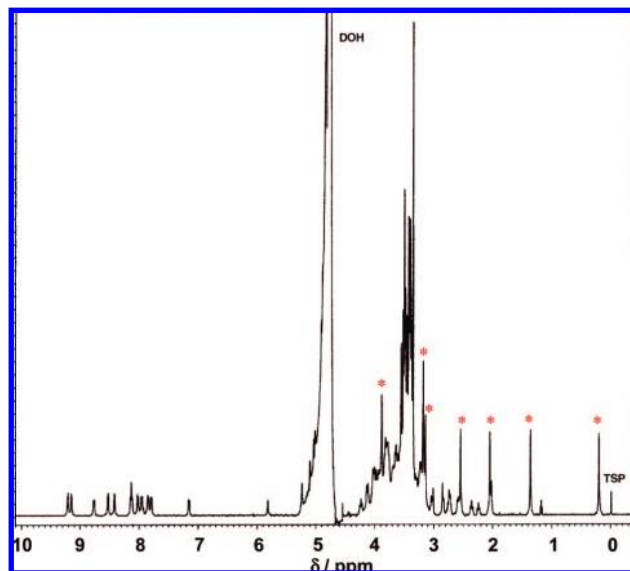
Figure 2. 500-MHz ^{1}H NMR spectrum of (CO)Fe(II)PCD ([Fe^{II}TPPS] = 5×10^{-3} M, [Py2CD] = 6×10^{-3} M) in 0.05 M phosphate buffer at pD 7.0 and 25 °C. The marked singlet signals are ascribed to the O-methyl protons at the secondary hydroxy group sides of Py2CD.

Figure 3. UV−vis spectra of Fe(II)PCD ([Fe^{II}TPPS] = 5.0×10^{-6} M, [Py2CD] = 6.0×10^{-6} M) under Ar, O$_2$, and CO atmospheres in 0.05 M phosphate buffer at pH 7.0 and 3 °C.

μ-oxo dimer weakened, and the band at 415 nm due to the inclusion complex of Fe^{III}TPPS and Py2CD strengthened (Supporting Information). The decrease and the increase in the absorbances at 408 and 415 nm, respectively, were saturated at one equivalent of Py2CD, indicating the formation of a very stable 1:1 complex ($K > 10^7$ M^{-1}). The formation of the μ-oxo dimer of Fe^{III}TPPS was completely inhibited by complexing with Py2CD.

The 1:1 complex of Fe^{III}TPPS and Py2CD (Fe(III)PCD) was definitely detected by ESI-MS spectroscopy (negative mode, pH 4.2) (Supporting Information). The MS peak was observed at $m/z = 1306$. Since the z value is 3, the molecular weight of the sample must be 3918 that corresponds to Fe(III)PCD (molecular weight = 3918.94). The isotope pattern of the spectrum is in complete agreement with the theoretical prediction.

We measured the ^{1}H NMR spectrum of the carbon monoxide adduct of the Fe^{II}TPPS−Py2CD complex ((CO)Fe(II)PCD, vide infra) that must be diamagnetic if the pyridine moiety in the linker of Py2CD coordinates to the Fe(II) center of Fe^{II}TPPS. Figure 2 shows the ^{1}H NMR spectrum of (CO)Fe(II)PCD in D$_2$O. Since all the proton signals were observed between 0 and 10 ppm, (CO)Fe(II)PCD should be a six-coordinate diamagnetic complex where the pyridine ligand in the linker of Py2CD coordinates to the Fe(II) center of Fe(II)PCD. The seven singlet signals due to the OCH$_3$ protons were observed at 0.208, 1.372, 2.059, 2.558, 3.154, 3.190, and 3.891 ppm. The HMBC spectrum (^{1}H-detected multibond heteronuclear multiple quantum coherence spectrum, Supporting Information) clearly indicates that these singlet signals are attributed to the *O*-methyl groups of Py2CD at the 2- and 3-positions. These results can only be explained by the structure of Fe(II)PCD shown in Figure 1, where the two cyclodextrin moieties include the sulfonatophenyl groups at the 5- and 15-positions of Fe^{II}TPPS. The structure of Fe(III)PCD can easily be deduced from that of (CO)Fe(II)PCD.

The spectroscopic pH titration of Fe(III)PCD indicated that the pK_a value for the equilibrium between the aqua-hydroxo complexes of Fe(III)PCD is 6.9. The λ_{max} values of
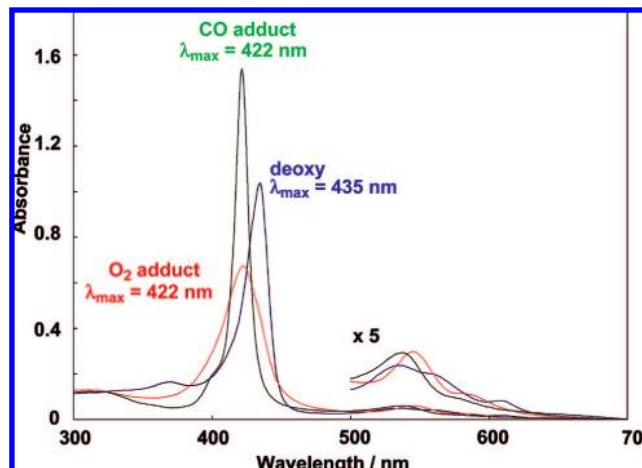
(H$_2$O)Fe(III)PCD and (OH$^-$)Fe(III)PCD were 400 and 415 nm, respectively.

Dioxygen Binding. In a glovebox with an Ar atmosphere, a mixture of Fe^{III}TPPS (0.82 μmol) and Py2CD (0.98 μmol) in 1 mL of N$_2$-saturated phosphate buffer at pH 7.0 was reduced by Na$_2$S$_2$O$_4$ (2.5 μmol), and the resulting solution was diluted by 3.0 mL using the same buffer solution, and then the UV−vis spectrum was measured (Figure 3). The λ_{max} of Fe(II)PCD was observed at 435 nm ($\varepsilon = 2.36 \times 10^5$ M^{-1} cm^{-1} at 25 °C), which shifted to 422 nm ($\varepsilon = 1.60 \times 10^5$ M^{-1} cm^{-1} at 3 °C) when the dioxygen gas was introduced into the Fe(II)PCD solution at 3 °C. In order to confirm that the species having the λ_{max} at 422 nm is the dioxygen adduct of Fe(II)PCD ((O$_2$)-Fe(II)PCD), carbon monoxide gas was introduced into the oxygenated solution. The absorption band at 422 nm then significantly sharpened. Such a spectral change indicates the formation of the carbon monoxide adduct ((CO)Fe(II)PCD) ($\varepsilon = 3.50 \times 10^5$ M^{-1}cm^{-1} at 25 °C). Since Na$_2$S$_2$O$_4$ was completely decomposed during the oxygenation of Fe(II)PCD, (CO)Fe(II)PCD must be the product through the ligand exchange of (O$_2$)Fe(II)PCD.

The ^{16}O$_2$−Fe stretching band of (O$_2$)Fe(II)PCD was observed at 568 cm^{-1} in the resonance Raman spectrum that shifted to 545 cm^{-1} when ^{16}O$_2$ was replaced with ^{18}O$_2$ (Supporting Information). Table 1 summarizes the Fe(II)−O$_2$ stretching frequencies of the native and artificial dioxygen receptors, and Chart 1 illustrates the structures. The peak wavenumber of (O$_2$)Fe(II)PCD (568 cm^{-1}) was in good agreement with those reported for native Mb (573 cm^{-1})[18] and Hb (568 cm^{-1})[19] as well as their model systems (563−586 cm^{-1}).[10,20−23] The Raman peak suggests that the strength of the Fe(II)−O$_2$ bond in

(18) Kerr, E. A.; Yu, N. T.; Bartnicki, D. E.; Mizukami, H. *J. Biol. Chem.* **1985**, *260*, 8360–8365.
(19) Hirota, S.; Ogura, T.; Appelman, E. H.; Shinzawa-Itoh, K.; Yoshikawa, S.; Kitagawa, T. *J. Am. Chem. Soc.* **1994**, *116*, 10564–10570.
(20) Walters, M. A.; Spiro, T. G.; Suslick, K. S.; Collman, J. P. *J. Am. Chem. Soc.* **1980**, *102*, 6857–6858.
(21) Desbois, A.; Momenteau, M.; Lutz, M. *Inorg. Chem.* **1989**, *28*, 825–834.
(22) Tani, F.; Matsu-ura, M.; Ariyama, K.; Setoyama, T.; Shimada, T.; Kobayashi, S.; Hayashi, T.; Matsuo, T.; Hisaeda, Y.; Naruta, Y. *Chem. Eur. J.* **2003**, *9*, 862–870.
(23) Kano, K.; Kitagishi, H.; Mabuchi, T.; Masahito, K.; Hirota, S. *Chem. Asian. J.* **2006**, *1*, 358–366.

Table 1. Fe(II)−O$_2$ Stretching Frequencies of Native and Artificial Dioxygen Receptors

O$_2$ receptor[a]	axial ligand	$\nu_{Fe(II)-^{16}O_2}$ ($\nu_{Fe(II)-^{18}O_2}$)/cm^{-1}	conditions	ref
Mb (sperm whale)	imidazole	573 (549)	pH 8.2	18
Mb (horse)	imidazole	571 (545)	pH 8.5	19
Hb (human)	imidazole	568 (544)	pH 8.5	19
Fe(TpivPP)(1-MeIm)	1-methylimidazole	568	CH$_2$Cl$_2$	20
Fe[(piv)2-Cn](1-MeIm)	1-methylimidazole	563	toluene	21
TCP-Im	imidazole	586 (560)	toluene	22
TCP-Py	pyridine	583 (558)	toluene	22
hemoCD1	pyridine	569 (546)	pH 7.0	10
Fe(II)ImCD	imidazole	573 (550)	pH 7.0	23
Fe(II)PCD	pyridine	568 (545)	pH 7.0	this work

[a] The structures of the O$_2$ receptors are shown in (Chart 1).

Chart 1. Structures of the Mb-Model Compounds
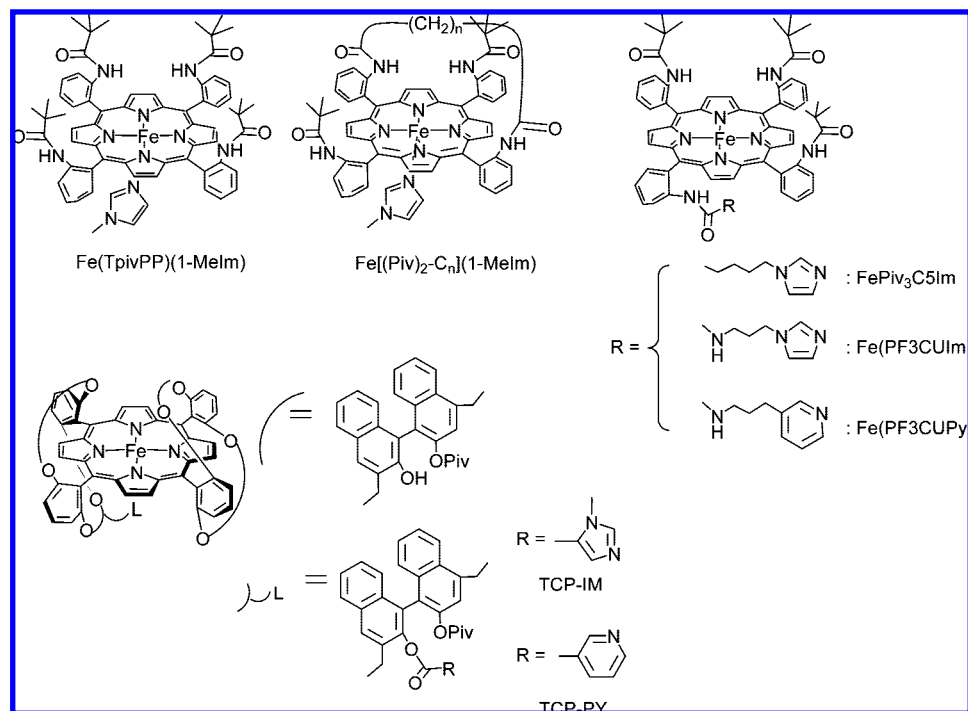
Table 2. Affinities and Kinetic Data for O$_2$ and CO Binding in Native and Artificial Systems

system[a]	$P_{1/2}{}^{O2}$/ Torr	$10^{-7}k_{on}{}^{O2}$/ M^{-1}s^{-1}	$10^{-3}k_{off}{}^{O2}$/ s^{-1}	$10^3 P_{1/2}{}^{CO}$/ Torr	$10^{-7}k_{on}{}^{CO}$/ M^{-1}s^{-1}	$10^2 k_{off}{}^{CO}$/ s^{-1}	$10^{-4}M^b$	ref
Mb	0.37−1.0	1−2	0.010−0.030	14−25	0.03−0.05	0.15−4	0.002−0.004	1a
Hb (human, R state)	0.22	3.3	0.0131	1.3	0.46	0.9	0.015	1a
FePiv$_3$5CIm	0.58	43	2.9	0.022	3.6	0.78	2.7	13
Fe(PF3CUIm)	1.26	26	3.9	0.049	2.9	1.4	2.6	24
Fe(PF3CUPy)	52.2	30	190	0.64	4.8	33	7.6	24
TCP-Im	1.3	4.0	2.0	1.1	2.1	23	0.118	22
TCP-PY	9.4	2.7	2.5	17	1.6	320	0.055	22
hemoCD1	16.9	4.7	1.3	0.015	1.3	0.025	110	8
Fe(II)ImCD	1.7	−	−	1.6	−	−	0.104	23
Fe(II)PCD	176	1.3	3.8	16	0.24	4.8	1.1	this work

[a] The structures of the iron porphyrins are shown in Chart 1 [b] $M = P_{1/2}{}^{O2}/P_{1/2}{}^{CO}$.

(O$_2$)Fe(II)PCD is almost the same as that of human Hb and weaker than that of Mb. The fact that the Raman stretching bands of the Fe(II)−O$_2$ bonds of the imidazole-coordinated model systems appear at higher wavenumbers as compared with those of the corresponding pyridine-coordinated ones suggests that the imidazole coordination to the Fe(II) center stabilizes the Fe(II)−O$_2$ bond more effectively than the pyridine coordination.

A dioxygen affinity of an O$_2$ receptor is usually represented by $P_{1/2}{}^{O2}$ (see Experimental Section). The $P_{1/2}{}^{O2}$ values of

Fe(II)PCD at 3 and 25 °C were determined to be 42.4 ± 1.6 and 176 ± 3 Torr, respectively. Table 2 shows the $P_{1/2}{}^{O2}$ values and the kinetic data for the native and artificial dioxygen receptors.[1a,8,13,22−24] The relatively poor ability of Fe(II)PCD to bind dioxygen is ascribed to the slower association of dioxygen to deoxy-Fe(II)PCD and the faster dissociation of dioxygen from (O$_2$)Fe(II)PCD. The $k_{on}{}^{O2}$ values for native Mb

(24) Collman, J. P.; Brauman, J. I.; Iverson, B. L.; Sessler, J. L.; Morris, R. M.; Gibson, Q. H. *J. Am. Chem. Soc.* **1983**, *105*, 3052–3064.
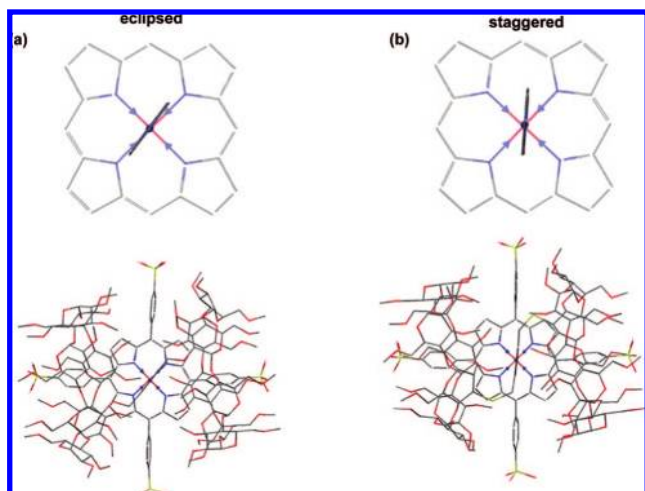
Figure 4. Energy-minimized structures of (a) Fe(II)PCD and (b) hemoCD1 obtained from the MM2 calculations using BioMedCAChe 6.0. The pyridine plain of Fe(II)PCD aligns on the straight line between the opposed pyrrole nitrogens of the porphyrin (eclipsed conformation), while that of hemoCD1 crosses the straight line (staggered conformation).

and Hb and the model system involving the apoprotein-like functionality (hemoCD1, Fe(II)ImCD, and Fe(II)PCD) are slower than those for the artificial dioxygen receptors (FePiv₃5CIm, Fe(PF3CUIm), and Fe(PF3CUPy) whose iron centers are directly exposed to the bulk phases. In an homogeneous system, the k_{on}^{O2} significantly depends upon the diffusion rate of O_2. In the hemoprotein, however, the k_{on}^{O2} is affected by more complex factors such as local concentration and orientation of dioxygen inside the heme pocket and penetration rate of dioxygen into the heme pocket. The situation of Fe(II)PCD as well as hemoCD1 is similar to that of the hemoprotein. Meanwhile, the k_{off}^{O2} is not affected by such a microenvironment. It must be difficult to compare the k_{off}^{O2} of Mb or Hb having a distal His with those of the artificial systems that lack the distal His. A comparison between Fe(II)PCD and hemoCD1 is preferable. We then noticed the orientation of the proximal pyridine that explains the difference in the O_2-binding kinetics between Fe(II)PCD and hemoCD1. The plane of the proximal His of Mb is aligned with the line connecting the nitrogen atom of a pyrrole with that of the opposite pyrrole ("eclipsed conformation"). Meanwhile, the plane of the proximal His of leghemoglobin crosses the line ("staggered conformation").[25] The computer simulation suggested that the staggered conformation stabilized the dioxygen adduct more effectively than the eclipsed one.[26] Therefore, the O_2-binding affinity of leghemoglobin is higher than that of Mb or Hb.[26] The molecular mechanics (MM) calculations for Fe(II)PCD showed that the pyridine unit coordinating to Fe(II) takes the "eclipsed conformation", while that in hemoCD1 takes the "staggered conformation" (Figure 4). The positions at which the pyridine linker is attached are the 2- and 2′- and 3-and 3′-positions of the cyclodextrin units of Py2CD and Py3CD, respectively. Such a difference may cause the difference in the conformations of the pyridine ligands between Fe(II)PCD and hemoCD1, leading to the difference in the O_2-binding affinities. The lower affinity of Fe(II)PCD can be interpreted in terms of the eclipsed

conformation of the pyridine ligand. The MM calculation also suggested that the inside of the capsule formed by the face-to-face cyclodextrin cavities of Fe(II)PCD does not have enough space to involve two or more dioxygen molecules.

The dioxygen of (O_2)Fe(II)PCD was released to form Fe(II)PCD upon replacement of the air atmosphere by N_2. Fe(II)PCD thus formed bound dioxygen again at 3 °C by bubbling air into the solution of deoxy-Fe(II)PCD, although a slight autoxidation occurred (Supporting Information). Vigorous air-bubbling enhanced the autoxidation of (O_2)Fe(II)PCD, while it was very stable upon standing. The bubbling probably causes vibration of the capsule formed by two cyclodextrin cavities resulting in opening and closing of the cleft of the capsule. Opening of the cleft of the capsule causes penetration of a water molecule into the capsule leading to the autoxidation of (O_2)Fe(II)PCD to Fe(III)PCD and the superoxide anion.[7,8]

As already mentioned above, (O_2)Fe(II)PCD was scarcely oxidized upon standing, although (O_2)hemoCD1 was gradually autoxidized with the half-lifetime ($t_{1/2}$) of 30 h at 25 °C.[8] Nonetheless, the kinetic measurement ($k_{off}^{O2} = 3.8 \times 10^3$ s⁻¹) indicated that (O_2)Fe(II)PCD is not stable. These findings can only be interpreted in terms of the tight encapsulation of oxygenated Fe^{II}TPPS by two cyclodextrin cavities of Py2CD resulting in a distinct "cage effect". Although dioxygen is kinetically released from (O_2)Fe(II)PCD at a relatively rapid rate, it cannot slip out of the Py2CD capsule and into the polar aqueous bulk phase due to the hydrophobic nature of dioxygen. The dioxygen remaining in the capsule rebinds with Fe^{II}TPPS inside the cage. The extremely long lifetime of (O_2)Fe(II)PCD indicates that the encapsulation of Fe^{II}TPPS by Py2CD is very tight and no penetration of a water molecule into the capsule proceeds unless the system is activated by some perturbation. In the case of the laser flash photolysis for determining k_{on}^{O2}, the dioxygen released from photoexcited (O_2)Fe(II)PCD may have a large kinetic energy resulting in extrusion of the dioxygen from the capsule of Fe(II)PCD. Therefore, the measured rate of the dioxygen association seems to involve the penetration of O_2 into the cyclodextrin capsule and the O_2-binding to the Fe(II) center inside the capsule.

Carbon Monoxide Binding. Carbon monoxide is strongly bound to the four- and five-coordinate iron(II) porphyrins.[27] The $P_{1/2}^{CO}$ for Fe(II)PCD was 0.016 Torr at 25 °C that is comparable to those for native Mb and is larger than that of human Hb in the R state (Table 2). The relatively low ability of Fe(II)PCD to bind carbon monoxide is ascribed to the fast dissociation rate of (CO)Fe(II)PCD. The labile nature of (CO)Fe(II)PCD was supported by the results of the resonance Raman spectroscopy. The Fe(II)−¹²C¹⁶O stretching band (ν_{Fe-CO}) of (CO)Fe(II)PCD was observed at 492 cm⁻¹ that shifted to 481 cm⁻¹ upon replacement of ¹²C¹⁶O with ¹³C¹⁸O. The C−O stretching bands of (CO)Fe(II)PCD were detected at 1984 and 1892 cm⁻¹ for ¹²C¹⁶O and ¹³C¹⁸O, respectively. Compared with the results of the resonance Raman spectroscopy for the CO-adducts of the native and artificial receptors (Supporting Information), (CO)Fe(II)PCD seems to be unstable when compared to other systems. We reported that the $P_{1/2}^{CO}$ of hemoCD1 is 1.5×10^{-5} Torr. The CO affinity of hemoCD1 is extremely higher than those for other systems (see Table 2). It has been reported that the dissociation rate of CO from (CO)Mb with the eclipsed

(25) Kundu, S.; Snyder, B.; Das, K.; Chowdhury, P.; Park, J.; Petrich, J. W.; Hargrove, M. S. *Proteins* **2002**, *46*, 268–277.

(26) Capece, L.; Marti, M. A.; Crespo, A.; Doctorivich, F.; Estrin, D. A. *J. Am. Chem. Soc.* **2006**, *128*, 12455–12461.

(27) (a) Olson, J. S.; Phillips, G. N., Jr. *J. Biol. Inorg. Chem.* **1997**, *2*, 544–552. (b) Springer, B. A.; Sligar, S. G.; Olson, J. S.; Phillips, G. N., Jr. *Chem. Rev.* **1994**, *94*, 699–714.

conformation of the proximal His ($k_{off}^{CO} = 1.9 \times 10^{-2}$ s^{-1}) is faster than that from the CO-adduct of leghemoglobin having the staggered conformation (8.4×10^{-3} s^{-1}).[28] The difference in the CO affinities between Fe(II)PCD and hemoCD1 can, at least in part, be interpreted in terms of the difference in the orientation of the pyridine ligand as in the case of the dioxygen binding. The results of the dioxygen and carbon monoxide binding demonstrate that Fe(II)PCD and hemoCD1 are the functional models of Mb and leghemoglobin, respectively.

Nitric Oxide Binding. Nitric oxide (NO) is a stable radical and is the most attractive diatomic molecule because of its multimodal biological functions.[29] Nitric oxide is biosynthesized from L-arginine (L-Arg) by the action of nitric oxide synthase (NOS)[30] and is bound to hemoproteins, such as cytochrome P450,[31] cytochrome *c* oxidase,[32] nitrile hydratase,[33] and catalase,[34] to inhibit the functions of these enzymes. Nitric oxide is scavenged by oxyMb[35] with a diffusion-controlled rate yielding metMb and the NO_3^- anion.[36] OxyHb also promotes the same oxidation of nitric oxide.[37] There are numerous studies of NO binding to the native hemoproteins and the artificial metalloporphyrins.[38] However, there is no example of NO binding and reactions in model systems involving the apoprotein functionality in an aerobic aqueous solution.

The NO-adduct of Fe(II)PCD was prepared by the reductive nitrosylation of Fe(III)PCD by nitric oxide[39] and conveniently purified by a Sephadex G-25 column. The λ_{max} of (NO)Fe-(II)PCD was observed at 420 nm ($\varepsilon_{max} = 1.85 \times 10^5$ M^{-1}cm^{-1}). Previously, we found that TMe-β-CD forms very stable 2:1 complexes of the TPPS free base and FeTPPS in which the two TMe-β-CD molecules include the sulfonatophenyl groups at the 5- and 15-positions of each porphyrin.[11,40] The Fe^{III}TPPS-TMe-β-CD complex also formed the NO adduct ((NO)Fe-
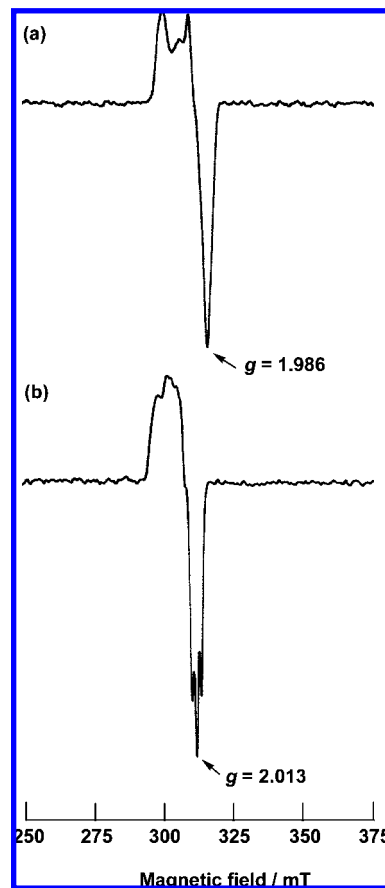
Figure 5. ESR spectra of (a) (NO)Fe(II)PCD (1.8×10^{-4} M) and (b) (NO)Fe(II)PTMCD (1.8×10^{-4} M) in 0.05 M phosphate buffer at pH 7.0 and 77 K. The NO-adducts were prepared by the reductive nitrosylation of Fe(III)PCD and Fe(III)PTMCD and purified by passing through the Sephadex G-25 columns.

(II)PTMCD) by reductive nitrosylation. The five-coordinate (NO)Fe(II)PTMCD showed a λ_{max} at 401 nm while that of (NO)Fe(II)PCD was 420 nm. The characteristic Soret bands of the five- and six-coordinate NO complexes of the ferrous porphyrins have been known to appear at around 400 and 420 nm, respectively.[41] The results of UV–vis spectroscopy suggest that (NO)Fe(II)PCD is a six-coordinate complex.

In order to further determine whether the pyridine ligand in (NO)Fe(II)PCD coordinates to the Fe(II) center, the EPR spectra of (NO)Fe(II)PCD and (NO)Fe(II)PTMCD were measured (Figure 5). In the case of (NO)Fe(II)PCD, a simple EPR signal without a hyperfine structure ($g = 1.986$) was observed. Meanwhile the hyperfine structure ($g = 2.013$) was detected in the spectrum of (NO)Fe(II)PTMCD. It is known that the five-coordinate NO complex of a ferrous porphyrin shows a hyperfine structure due to the spin coupling of the lone pair electron of nitric oxide with a ^{14}N nucleus, while the hyperfine structure becomes obscure in the six-coordinate NO complex whose g-value is smaller than that of the five-coordinate one.[42] The EPR spectrum of (NO)Fe(II)PCD proves that the pyridine ligand coordinates to the Fe(II) center. The NO–Fe(II) bonds

(28) Kundu, S.; Blouin, G. C.; Premer, S. A.; Sarath, G.; Olson, J. S.; Hargrove, M. S. *Biochemistry* **2004**, *43*, 6241–6252.

(29) (a) Bonner, F. T.; Stedman, G. In *Methods in Nitric Oxide Research*; Feelisch, M., Stamler, J. S., Eds.; John Wiley & Sons: Chichester, U.K., 1996; pp 3–18. (b) Stamler, J. S.; Feelisch, M. In *Methods in Nitric Oxide Research*; Feelisch, M., Stamler, J. S., Eds.; John Wiley & Sons: Chichester, U.K., 1996; pp 19–18.

(30) (a) Palacios, M.; Knowles, R. G.; Palmer, R. M. J.; Moncada, S. *Biochem. Biophys. Res. Commun.* **1989**, *165*, 802–809. (b) Bredt, D. S.; Hwang, P. M.; Snyder, S. H. *Nature* **1990**, *347*, 768–770. (c) Bredt, D. S.; Snyder, S. H. *Proc. Natl. Acad. Sci. U.S.A.* **1990**, *87*, 682–685. (d) Radomski, M. W.; Palmer, R. M.; Moncada, S. *Br. J. Pharmacol.* **1990**, *101*, 325–328. (e) Radomski, M. W.; Palmer, R. M. J.; Moncada, S. *Proc. Natl. Acad. Sci. U.S.A.* **1990**, *87*, 5193–5197.

(31) Minamiyama, Y.; Takemura, S.; Imaoka, S.; Funae, Y.; Tanimoto, Y.; Inoue, M. *J. Pharmacol. Exp. Ther.* **1997**, *283*, 1479–1485.

(32) Cleeter, M. W. J.; Cooper, J. M.; Darley-Usmar, V. M.; Moncada, S.; Schapira, A. H. V. *FEBS Lett.* **1994**, *345*, 50–54.

(33) Tsujimura, M.; Dohmae, N.; Odaka, M.; Chijimatsu, M.; Takio, K.; Yohda, M.; Hoshino, M.; Nagashima, S.; Endo, I. *J. Biol. Chem.* **1997**, *272*, 29454–29459.

(34) Brown, G. C. *Eur. J. Biochem.* **1995**, *232*, 188–191.

(35) Giulivi, C.; Kato, K.; Cooper, C. E. *Am. J. Physiol.* **2006**, *291*, C1225–C1231.

(36) (a) Herold, S.; Exner, M.; Nauser, T. *Biochemistry* **2001**, *40*, 3385–3395. (b) Ford, P. C. *Pure Appl. Chem.* **2004**, *76*, 335–350.

(37) (a) Caccia, S.; Denisov, I.; Perrella, M. *Biophys Chem.* **1999**, *76*, 63–72. (b) Joshi, M. S.; Ferguson, T. B., Jr.; Han, T. H.; Hyduke, D. R.; Liao, J. C.; Rassaf, T.; Bryan, N.; Feelisch, M.; Lancaster, J. R., Jr. *Proc. Natl. Acad. Sci. U.S.A.* **2002**, *99*, 10341–10346.

(38) (a) Hoshino, M.; Laverman, L.; Ford, P. C. *Coord. Chem. Rev.* **1999**, *187*, 75–102. (b) Ford, P. C.; Lorkovic, I. M. *Chem. Rev.* **2002**, *102*, 993–1017. (c) Møller, J. K. S.; Skibsted, L. H. *Chem. Rev.* **2002**, *102*, 1167–1178. (d) Ford, P. C. *Pure Appl. Chem.* **2004**, *76*, 335–350.

(39) Fernandez, B. O.; Lorkovic, I. M.; Ford, P. C. *Inorg. Chem.* **2004**, *43*, 5393–5402.

(40) Kano, K.; Nishiyabu, R.; Asada, T.; Kuroda, Y. *J. Am. Chem. Soc.* **2002**, *124*, 9937–9944.

(41) Praneeth, V. K. K.; Näther, C.; Peters, G.; Lehnest, N. *Inorg. Chem.* **2006**, *45*, 2795–2811.

(42) (a) Praneeth, V. K. K.; Haupt, E.; Lehnert, N. *J. Inorg. Biochem.* **2005**, *99*, 940–948. (b) Voegtle, H. L.; Sono, M.; Adak, S.; Pond, A. E.; Tomita, T.; Derera, R.; Goodin, D. B.; Ikeda-Saito, M.; Stuehr, D. J.; Dawson, J. H. *Biochemistry* **2003**, *42*, 2475–2484.
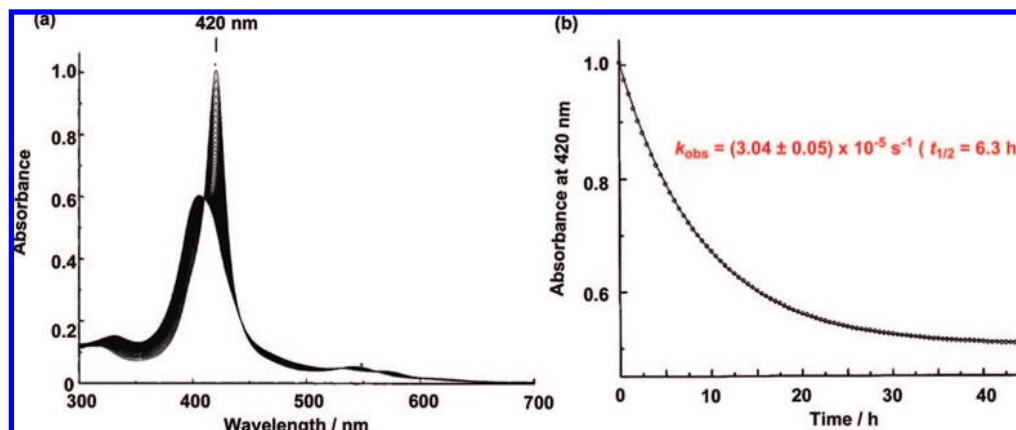
Figure 6. (a) UV−vis absorption spectral changes in oxidation reaction of (NO)Fe(II)PCD (5.5×10^{-6} M) to Fe(III)PCD under air in 0.05 M phosphate buffer at pH 7.0 and 25 °C. Scans were carried out at 0.5-h intervals. (b) Time courses in absorbance at 420 nm of (NO)Fe(II)PCD. The solid line is the theoretical curve.

of the six-coordinate NO complexes of the ferrous porphyrins are known to be much less stable than those of the five-coordinate ones because of the back bonding from Fe(II) to NO promoted by the proximal base.[38a,41,43] In our model system, the proximal pyridine does not dissociate even when NO is bound to the Fe(II) center.

The oxidation of the dioxygen adducts of the ferrous porphyrins by nitric oxide has been well studied because of the relation with the nitric oxide regulation by oxyMb. The peroxynitrite-coordinate porphyrins have been established as the intermediates (eq 3) [36a,44]

$$\underset{Fe^{II}}{\overset{\overset{O}{\underset{|}{O}}}{\bigcirc}} \quad \xrightarrow{NO} \quad \underset{Fe^{II}}{\overset{\overset{O-N=O}{\underset{|}{O}}}{\bigcirc}} \quad \longrightarrow \quad \underset{Fe^{III}}{\bigcirc} + NO_3^- \qquad (3)$$
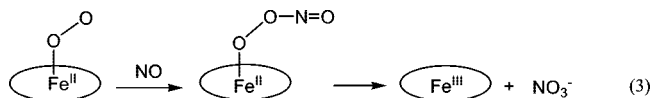
Meanwhile, there are a few studies on the oxidation of the NO adducts of the ferrous porphyrins. Nitrosyl Mb and Hb have been assumed to be oxidized via slow ligand-exchanges between NO and O_2 yielding oxyMb and oxyHb, respectively, which react with released NO to yield the met-forms of the hemoproteins and the NO_3^- anion.[45,46] Meanwhile, the nitrosylated heme bound to hemopexin has been demonstrated to be oxidized by dioxygen via an intermediate involving the $Fe^{II}-NO(OO)$ bond that slowly converts to a hemin−hemopexin complex and the NO_3^-.[47] The Fe(II) centers of (NO)Mb, (NO)Hb, and the (NO)heme−hemopexin complex are all coordinated by the proximal His. The present study is the first example of the oxidation of the six- and five-coordinate NO-adducts of a ferrous porphyrin in a model system in aerobic aqueous solution.

The oxidation of (NO)Fe(II)PCD to Fe(III)PCD and NO_3^- gradually occurred under the aerobic conditions (Figure 6). The pseudo-first-order rate constant for the oxidation of (NO)Fe(II)PCD was $(3.04 \pm 0.05) \times 10^{-5}$ s^{-1} in 0.05 M phosphate buffer at pH 7.0 and 25 °C. The $t_{1/2}$ of (NO)Fe(II)PCD was 6.3 h. In the case of native Mb, the oxidation of (NO)Mb has been reported to occur

(43) Kharitonov, V. G.; Sharma, V. S.; Magde, D.; Koesling, D. *Biochemistry* **1997**, *36*, 6814–6818.
(44) Eich, R. F.; Li, T.; Lemon, D. D.; Doherty, D. H.; Curry, S. R.; Aitken, J. F.; Mathews, A. J.; Johnson, K. A.; Smith, R. D.; Phillips, G. N., Jr.; Olson, J. S. *Biochemistry* **1996**, *35*, 6976–6983, and references therein.
(45) Møller, J. K. S.; Skibsted, L. H. *Chem. Eur. J.* **2004**, *10*, 2291–2300.
(46) Herold, S.; Röck, G. *Biochemistry* **2005**, *44*, 6223–6231.
(47) Fasano, M.; Antonini, G.; Ascenzi, P. *Biochem. Biophys. Res. Commun.* **2006**, *345*, 704–712.

Figure 7. Plot of k_{obs} versus O_2 partial pressure (P_{O2}) in N_2 for oxidation of (NO)Fe(II)PCD. The k_{obs}'s were measured in 0.05 M phosphate buffer at pH 7.0 and 25 °C.

in two consecutive pseudo-first-order reactions due to the ligand exchange between NO and O_2 and the subsequent reaction of oxyMb with nitric oxide, the k_1 and k_2 values being $(2.46 \pm 0.11) \times 10^{-4}$ and $(3.96 \pm 0.22) \times 10^{-4}$ s^{-1}, respectively, at 25 °C.[45] In our model system, however, only a single exponential decay of the NO-adduct was observed. Figure 7 shows the effects of the dioxygen partial pressure (P_{O2}) on the oxidation of (NO)Fe(II)PCD. The k_{obs} value increased with increasing P_{O2} at a lower P_{O2} and saturated at a higher P_{O2}. From the results shown in Figure 7, the maximum rate constant for the oxidation (k_{max}) was estimated to be $(5.12 \pm 0.18) \times 10^{-5}$ s^{-1}.

The rate of the dissociation of nitric oxide from (NO)Fe(II)PCD was measured by a typical method.[46–48] Namely, the conversion of (NO)Fe(II)PCD to (CO)Fe(II)PCD was followed by the UV−vis spectral changes of the system in phosphate buffer at pH 7.0 and 25 °C containing $Na_2S_2O_4$ under the CO atmosphere (Supporting Information). The k_{off}^{NO} of (NO)Fe(II)PCD was determined to be $(5.58 \pm 0.42) \times 10^{-5}$ s^{-1}, which corresponds to the k_{max} for oxidation of (NO)Fe(II)PCD. In a solution containing a sufficient amount of O_2, free Fe(II)PCD formed via dissociation of NO from (NO)Fe(II)PCD immediately binds the dioxygen to form (O_2)Fe(II)PCD, which rapidly reacts with NO remaining inside the

(48) Moore, E. G.; Gibson, Q. H. *J. Biol. Chem.* **1976**, *251*, 2788–2794.

Scheme 1. Mechanism for oxidation of (NO)Fe(II)PCD
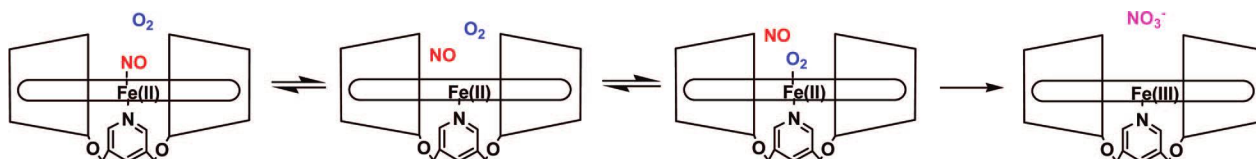
cavity to afford Fe(III)PCD and NO_3^- (Scheme 1). If nitric oxide released from (NO)Fe(II)PCD rapidly diffuses, the formation of (O_2)Fe(II)PCD must spectroscopically be observed. It is assumed that hydrophobic nitric oxide hardly slips out of the hydrophobic cavity and into the polar bulk phase resulting in a rapid reaction with (O_2)Fe(II)PCD inside the cavity. Since the capsule of Fe(II)PCD does not have enough space to contain both O_2 and NO, the oxidation of NO by O_2 might occur almost simultaneously with the binding of O_2 to the Fe(II) center. In the case of native (NO)Mb, the oxidation of NO by oxyMb slowly proceeds, suggesting that nitric oxide released from the adduct can diffuse in the protein through a hydrophobic route as does carbon monoxide.[49]

The temperature dependence of the oxidation of (NO)Fe-(II)PCD provided the activation enthalpy ($\Delta H^{\ddagger}$) and entropy changes ($\Delta S^{\ddagger}$) of 98.9 ± 2.6 kJ mol^{-1} and 0.17 ± 8.7 J mol^{-1} K^{-1}, respectively (Supporting Information). The large $\Delta H^{\ddagger}$

reflects the endothermic dissociation of the NO–Fe(II) bond. The $\Delta S^{\ddagger}$ value of the present system is almost zero, suggesting that no bimolecular interaction occurs in the transition state of the rate-determining step. In other words, the unimolecular dissociation process is the rate-determining step. The thermodynamic aspect supports the mechanism shown in Scheme 1.

Surprisingly, (NO)Fe(II)PTMCD was not oxidized at all under aerobic conditions. Although we followed the UV–vis spectral change for long periods of time, no spectral change was observed even at 40 h after the sample preparation. Meanwhile, the naked nitric oxide adduct of Fe^{II}TPPS ((NO)Fe^{II}TPPS), which was prepared in a glovebox, decomposed relatively rapidly. The UV–vis spectral changes of (NO)Fe^{II}TPPS in an aerobic buffer solution at pH 7.0 were so complex that no kinetic analysis could be carried out (Supporting Information). Within 10 min, most of the (NO)Fe^{II}TPPS molecules decomposed to yield unknown product(s) having a broad and weak band centered at ca. 410 nm. The ring-opening reaction of FeTPPS probably occurred. Such a marked difference in reactivity between (NO)Fe(II)PTMCD and (NO)Fe(II)TPPS cannot be explained at the present time.

Nitrosylation of Manganese Porphyrin. In order to examine whether the dioxygen adduct formation is essential for the oxidation of the nitric oxide adduct of a metalloporphyrin, we studied the oxidation of (NO)Mn^{II}TPPS encapsulated by Py2CD ((NO)Mn(II)PCD) because Mn(II)PCD does not form a stable dioxygen adduct at room temperature. Although the formation of the diamagnetic nitric oxide adduct of Mn^{II}TPP (TPP = 5,10,15,20-tetraphenylporphyrin dianion) has been reported,[53] no detailed studies on the nitrosyl Mn(II) porphyrins have been carried out. To the best of our knowledge, the present study is the first example of the oxidation of the nitrosyl Mn(II) porphyrin.

Figure 8 shows the progressive UV–vis spectral changes of (NO)Mn(II)PCD in aerobic phosphate buffer at pH 7.0 and 25 °C. (NO)Mn(II)PCD with its λ_{max} at 428 nm was very slowly oxidized to Mn(III)PCD (471 nm). The oxidation of (NO)Mn(II)PCD obeyed the zero-order kinetics. The half-lifetime ($t_{1/2}$) of (NO)Mn(II)PCD was 35 h, while that of (NO)Fe(II)PCD was 6.3 h. We also examined the autoxidation of (NO)Mn-(II)PTMCD without a proximal base and found that the zero-ordered oxidation proceeds much faster ($t_{1/2} = 5.0$ h) than that of (NO)Mn(II)PCD (Supporting Information). In this case, the formation of Mn(II)PTMCD ($\lambda_{max} = 434$ nm) produced by the release of nitric oxide from (NO)Mn(II)PTMCD was observed
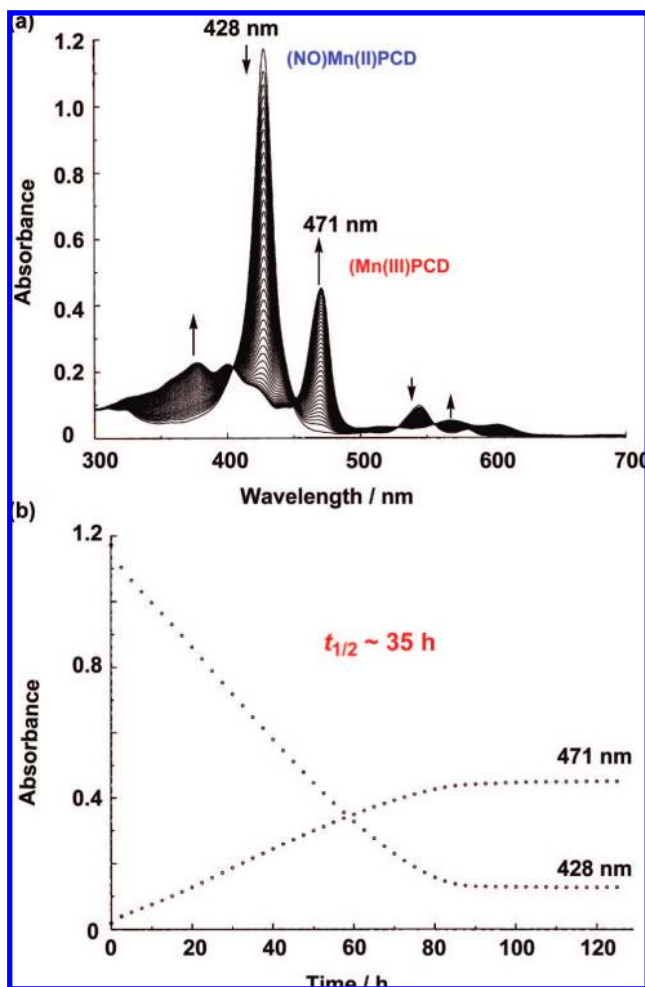
Figure 8. (a) UV–vis spectral changes in oxidation reaction of (NO)Mn(II)PCD (5.0×10^{-6} M) to Mn(III)PCD under air in 0.05 M phosphate buffer at pH 7.0 and 25 °C. Scans were carried out at 2.5-h intervals. (b) Time courses in absorbance at 428 and 471 nm.

(49) Nishihara, Y.; Sakakura, M.; Kimura, Y.; Terazima, M. *J. Am. Chem. Soc.* **2004**, *126*, 11877–11888, and references therein.
(50) Franke, A.; Stochel, G.; Suzuki, N.; Higuchi, T.; Okuzono, K.; van Eldik, R. *J. Am. Chem. Soc.* **2005**, *127*, 5360–5375.
(51) Laverman, L. E.; Ford, P. C. *J. Am. Chem. Soc.* **2001**, *123*, 11614–11622.
(52) Kikugawa, K.; Hiramoto, K.; Ohkawa, T. *Biol. Pharm. Bull.* **2004**, *27*, 17–23.
(53) (a) Wayland, B. B.; Olson, L. W. *Inorg. Chim. Acta* **1974**, *11*, L23–L24. (b) Wayland, B. B.; Olson, L. W.; Siddiqui, Z. U. *J. Am. Chem. Soc.* **1976**, *98*, 94–98.

Scheme 2. Reaction Mechanism for Oxidation of (NO)Mn(II)PCD
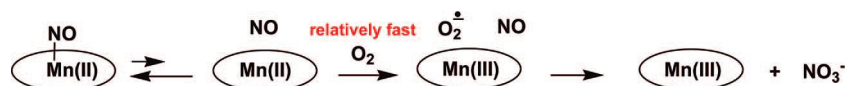
together with the advance of the oxidation. Mn(II)PTMCD gradually disappeared with the progress of the oxidation. If the equilibrium A $\rightleftharpoons$ B exclusively shifts to A, and a very small amount of B existing in the system relatively rapidly reacts to yield a final product, such a reaction obeys zero-order kinetics. We assumed the reaction mechanism for the autoxidation of (NO)Mn(II)PCD as shown in Scheme 2. In order to confirm the autoxidation of Mn(II)PCD without nitric oxide as the axial ligand to Mn(III)PCD, the progressive UV–vis spectral changes of Mn(II)PCD were followed in phosphate buffer under aerobic conditions (Supporting Information). Although the spectral changes with the fine isosbestic points were observed, the autoxidation did not obey the first-order kinetics. Anyway, the autoxidation of Mn(II)PCD ($t_{1/2}$ = ca. 5.8 h) proceeded more rapidly than the oxidation of (NO)Mn(II)PCD ($t_{1/2}$ = 35 h). The autoxidation of Mn(II)PTMCD was much faster ($t_{1/2}$ = 1.7 h). These findings provide two conclusions:

(1) The proximal base, pyridine, of Mn(II)PCD stabilizes the NO-adduct of this porphyrin while that of Fe(II)porphyrin destabilizes it.

(2) The rate-determining step of the oxidation of (NO)Mn-(II)PCD is the dissociation of nitric oxide from the adduct, which is the same as that for (NO)Fe(II)PCD.

The effect of the proximal base on stabilization of the NO-adduct on Mn(II)porphyrin is not sufficiently understood. However, it is known that a non-native soluble guanylyl cyclase (sGC) whose prosthetic group is substituted by Mn(II)PPIX (PPIX = protoporphyrin IX dianion) does not release the proximal His upon the binding of nitric oxide, while native sGC having Fe(II)PPIX as the prosthetic group removes its proximal His.[54] In the model system, the Fe(II)-axial base distance of nitrosyl Fe(II)TPP coordinated by 4-methylpiperidine has been known to be longer than the Mn(II)-base distance of the corresponding Mn(II)TPP complex.[55] The results of the autoxidation of (NO)Mn(II)PCD strongly support the mechanism shown in Scheme 1 that explains the autoxidation of (NO)Fe(II)PCD.

Conclusions

The MM calculations suggest that the proximal pyridine of Fe(II)PCD takes the "eclipsed conformation" that is similar to the orientation of the proximal His in native Mb or Hb, while that of hemoCD1 takes the "staggered conformation" that resembles the orientation of native leghemoglobin. If such calculations represent the real orientations of the pyridine moieties in these two model systems, the dioxygen affinity of Fe(II)PCD as a model of Mb or Hb should be lower than that of hemoCD1 as a model of leghemoglobin. The $P_{1/2}{}^{O2}$ for Fe(II)PCD is 176 Torr at 25 °C, while that for hemoCD1 is 17 Torr. The computational prediction is in good agreement with the experimental results, suggesting that

we have now acquired accurate model systems of Mb or Hb and leghemoglobin that work in aqueous solutions. Although the dioxygen affinity of Fe(II)PCD is lower than that of hemoCD1, the (O₂)Fe(II)PCD is not autoxidized in the still-standing, while (O₂)hemoCD1 is gradually autoxidized by the nucleophilic attack of a water molecule on the Fe(II)–O₂ bond ($t_{1/2}$ of (O₂)hemoCD1 = 30 h).[8] The extremely stable nature of (O₂)Fe(II)PCD can be interpreted in terms of the pronounced "cage effect". Fe(II)TPPS is completely and tightly encapsulated by the two cyclodextrin cavities of Py2CD leading to complete extrusion of the water molecules from the cage. Although the dioxygen molecule easily dissociates from (O₂)Fe(II)PCD, the released dioxygen cannot slip out of the cavity, thus resulting in the recombination with Fe(II)TPPS inside the cage. The same cage effects explain the behavior of Fe(II)PCD for the binding of carbon monoxide and nitric oxide. Although the naked Fe(II)TPPS is labile in an aerobic aqueous solution in the presence of nitric oxide, Fe(III)PCD affords the stable nitric oxide adduct of Fe(II)PCD through reductive nitrosylation. (NO)Fe(II)PCD is gradually oxidized to Fe(III)PCD and NO₃⁻ under the aerobic conditions. The $t_{1/2}$ of the six-coordinate (NO)Fe-(II)PCD with the axial base (pyridine) is 6.3 h, while the five-coordinate (NO)Fe(II)PTMCD does not decompose ($t_{1/2} \doteq \infty$), indicating the pyridine ligand of (NO)Fe(II)PCD weakens the Fe(II)–NO bond by donating the electron to the iron center. The kinetic study demonstrates that the rate-determining step of the autoxidation of (NO)Fe(II)PCD is the ligand-exchange reaction affording (O₂)Fe(II)PCD that immediately reacts with the released nitric oxide. Such a mechanism is supported by the results of the autoxidation of (NO)Mn(II)PCD that obeys zero-order kinetics.

Supporting Information Available: UV–vis spectral changes in the reaction of NO with hemoCD1, plot of k_{obs} for dioxygen association with Fe(II)PCD versus [O₂], UV–vis spectroscopic titration for determining binding constant for complexation of Fe^{III}TPPS with Py2CD, ESI-MS of Fe(III)PCD, HMBC spectrum of (CO)Fe(II)PCD, resonance Raman spectra of (¹⁶O₂)-Fe(II)PCD and (¹⁸O₂)Fe(II)PCD, UV–vis spectroscopic evidence for reversibility of dioxygen binding to Fe(II)PCD, resonance Raman frequencies of CO-adducts of various ferrous porphyrins, UV–vis spectral changes in dissociation of NO from (NO)Fe(II)PCD under CO atmosphere, Eyring plot for oxidation of (NO)Fe(II)PCD to Fe(III)PCD and NO₃⁻, UV–vis spectral changes in decomposition of (NO)Fe(II)TPPS in aerobic phosphate buffer, UV–vis spectral changes in oxidation of (NO)Mn(II)PTMCD, UV–vis spectral changes in autoxidation of Mn(II)PCD without NO ligand to Mn(II)PCD in aerobic phosphate buffer. This material is available free of charge via the Internet at http://pubs.acs.org.

JA8009583

(54) Dierks, E. A.; Hu, S.; Vogel, K. M.; Yu, A. E.; Spiro, T. G.; Burstyn, J. N. *J. Am. Chem. Soc.* **1997**, *119*, 7316–7323.
(55) (a) Scheidt, W. R.; Brinegar, A. C.; Ferro, E. B.; Kirner, J. F. *J. Am. Chem. Soc.* **1977**, *99*, 7315–7322. (b) Piciulo, P. L.; Rupprecht, G.; Scheidt, W. R. *J. Am. Chem. Soc.* **1974**, *96*, 5293–5295. (c) Scheidt, W. R.; Hatano, K.; Rupprecht, G. A.; Piciulo, P. L. *Inorg. Chem.* **1979**, *18*, 292–299.